CHEMICAL ENGINEERING TRANSACTIONS
VOL. 94, 2022
A publication of AIDIC
The Italian Association of Chemical Engineering
Online at www.cetjournal.it
Guest Editors: Petar S. Varbanov, Yee Van Fan, Jiří J. Klemeš, Sandro Nižetić

**ISBN** 978-88-95608-93-8; **ISSN** 2283-9216
DOI: 10.3303/CET2294047

# Experimental Investigation and Modelling of PSA Oxygen Generator in Context of Oxy-fuel Combustion

Marek Nedoma[a,*], Michal Netušil[b], Pavel Ditl[b]

[a]Czech Technical University in Prague, Faculty of Mechanical Engineering, Department of Energy Engineering, Technická 1902/4, 160 00 Prague 6, Czech Republic
[b]Czech Technical University in Prague, Faculty of Mechanical Engineering, Department of Process Engineering, Technická 1902/4, 160 00 Prague 6, Czech Republic
Marek.Nedoma@fs.cvut.cz

Oxy-fuel combustion is an attractive way toward low-carbon energy systems and carbon capture and storage (CCS) policy. Its economy largely depends on high-purity oxygen ($O_2$) price. The most commonly used commercial $O_2$ production technologies are cryogenic distillation (ASU), adsorption, and polymeric membrane separation. Pressure swing adsorption (PSA) is suitable for small and medium-sized $O_2$-consuming processes, which may be ideal for pilot-scale oxy-fuel plants. This paper generally investigates the performance of a two-bed four-step commercial PSA oxygen generator, quality and quantity of $O_2$ production, process scheduling, and optimal operating conditions. The air flow rate at ambient temperature and pressure of 8.5 - 11 bar ranged from 13 - 17 $m^3$ (STP)/h throughout the experiments. Furthermore, the textural properties of UOP PSAO2 XP molecular sieve with enhanced $N_2/O_2$ selectivity were experimentally determined and an increased presence of micropores was detected. To describe the process, an analytical flow-balance model was developed. This model calculates air factor (AirF), $O_2$ recovery (REC) and purity (PUR), and energy consumption based on the actual gas flow determined for the system, incorporates parameters sensitivity analysis, and verifies the PSA performance. The model was validated under four $O_2$ purity levels with the lowest measurement error. The experimental data obtained showed good agreement with the model results; the controversy surrounding some of the data is discussed. In practice, the application of the validated model provides an easy-to-grasp engineering solution.

## 1. Introduction

Air separation is the leading method for producing high purity $O_2$ to be used in the medical, energy, and manufacturing industries. In the energy industry, low-purity streams (25 - 40 %) are used for natural gas combustion, mid-purity streams are used in hybrid oxy-fuel combustion and post-combustion processes (up to 70 %), and high-purity streams of 90 % serve as a gasification medium in coal gasification and of 95 % as an oxidant in oxy-fuel combustion. Oxy-fuel is an important low-carbon technology. The high concentration of carbon dioxide ($CO_2$) in the flue gas allows efficient separation of high-purity $CO_2$. The high cost of $O_2$ production affects the economics of the process (Micari and Agrawal, 2022).
There are three commercial technologies to generate $O_2$. ASU is ill-conditioned for low $O_2$ production and is used exclusively in heavy industry to produce more than 150 $t_{O2}$/day carrying high PUR and REC values reaching 99.5 % and 98 %. Pressure and temperature swing adsorption technologies have been an industrial technology for several decades, generating small- to medium-sized supplies of $O_2$ (< 100 $t_{O2}$/d) with up to 95 % PUR at 30 % REC, as a standard (Wu et al., 2018). Polymeric membranes as a standalone technology achieve low PUR of 30 - 50 %, and a minimum capacity of 10 - 25 $t_{O2}$/d. Such streams can provide energy savings in natural gas combustion or can be used as a front-end $O_2$ enrichment in combined systems. Commercial membranes do not achieve sufficient $N_2/O_2$ selectivity and permeability, obtaining high PUR requires additional stages, use of ion conductive materials, or facilitated transport membranes (Micari and Agrawal, 2022). In the past decade, chemical looping air-separation (CLAS) has been studied, but the level of development is low (Krzystowczyk et al., 2021). An integration of CLAS in industry was initially discussed by Tang and You (2018).

Paper Received: 14 April 2022; Revised: 07 June 2022; Accepted: 21 July 2022
Please cite this article as: Nedoma M., Netušil M., Ditl P., 2022, Experimental Investigation and Modelling of PSA Oxygen Generator in Context of Oxy-fuel Combustion, Chemical Engineering Transactions, 94, 283-288 DOI:10.3303/CET2294047

Pairing oxy-fuel with CLAS showed better economics than conventional oxy-fuel combustion with ASU for different CCS scenarios. A standalone ASU accounts for 6 - 10 % of the power plant energy penalty. This value is about two times higher than the energy penalty of the $CO_2$ compression unit, the other auxiliary system of CCS technology (Yadav and Mondal, 2022).
PSA has been applied for $O_2$ separation from the beginning of its invention by Skarstrom in 1957, which he patented in 1960 (Skarstrom, 1960). Technology later adapted in industry to produce high-purity hydrogen and methane on a large-scale, remove carbon monoxide in plants, and supply $O_2$ on a small-scale (Wiessner, 1988). Small- to medium-scale $O_2$ production persists to this day in the fields of wastewater treatment, pulp and paper industries, and medicine. PSA is considered among possible alternatives to cryogenic separation, but low selectivity and sorption properties of adsorbents need improvement (Wu et al., 2018). Zeolites NaA and NaX are the most common adsorbents. They can separate $O_2$ with 95 % PUR; merely argon (Ar) is not separated. Large $O_2$ production is achieved by vacuum-pressure swing processes (Linde, 2019). It was demonstrated that a single-stage PSA based on the Skarstrom cycle can achieve PUR of 99.5 % with 5 % REC when using Ar-selective X-zeolite (Santos et al, 2007). However, using a second stage to separate Ar and residual $N_2$ from $O_2$ seems more reasonable for PSA-based cycles, as this technology is adopted for on-site $O_2$ production by manufacturers, for example, AirSep Corporation (up to 0.5 $t_{O2}$/d), Novair Industries (up to 0.55 $t_{O2}$/day) or Texas Compression Services (up to 0.8 $t_{O2}$/d). Other ways to improve PSA performance are to reduce energy consumption and enhance cycle productivity. It can be done, for example, by appropriate choice of pressure difference between the adsorbate and $O_2$ purge gas (Gizicki and Banaszkiewicz, 2020) and processes parameters, that is, working pressure and temperature, cycle duration, and reflux ratio (Skvortsov et al., 2018). An easy-to-operate oxy-fuel pilot-scale facilities with thermal power in the range of 0.1 - 3 $MW_{th}$ provide most opportunities for testing. Industrial-scale units without CCS technology have power over 10 $MW_{th}$, the pilot units demonstrating commercial oxy-fuel plants with CCS use burners with power exceeding 30 $MW_{th}$ in total; any larger oxy-fuel CCS projects are still in development (Lian and Zhang, 2018). Šulc and Ditl (2021) conducted a techno-economic study for utilisation of a two-bed Skarstrom-type PSA $O_2$ generator in a small bubbling fluidised bed oxy-combustor (0.5 $MW_{th}$). For local energy prices and supply of 0.61 $t_{O2}$/day with 95 % PUR, PSA with $O_2$ production cost of 0.115 EUR/kg of $O_2$ turned out to be approximately equal to that of liquid oxygen delivery.
The lack of studies on commercially available PSA technologies led to the investigation of operating principle of such technology using novel adsorbent for which detailed data are not yet available. The aim was to establish a solid understanding of this process for the subsequent optimisation and the scale-up study for a pilot-scale oxy-fuel plant. This required performing sets of experimental measurements, developing a simple model, and adsorbent characterisation to identify the benefits of a commercially available process. The experiments were carried out on a small-scale commercial PSA Skarstrom-type $O_2$ generator by Oxywise. The chosen approach was: (i) comparison of PUR dependence with the selected process metrics (REC, bed-size factor (BSF), and energy consumption), (ii) verification of the experimental results reliability along with sensitivity analysis of process parameters that may deteriorate the quantity and cost of $O_2$ production, which are of key importance to any oxy-fuel plant.

## 2. Methodology

### 2.1 Adsorbent

A commercial sample of porous zeolite molecular sieve UOP MOLSIV™ PSAO2 XP (UOP LLC, Honeywell) with enhanced $N_2/O_2$ selectivity was used. Adsorbent particles are homogeneous spheres of 2 mm diameter (8×12 mesh) with a bulk density of 656.8 kg/m$^3$. Textural properties were investigated by physical adsorption of argon at 87 K and nitrogen at 77 K (three-parameter BET and t-plot methods). Both adsorption isotherms of pure Ar and $N_2$ were measured using ASAP 2020 (Micromeritics). The results of the textural analysis are tabulated in Table 1 and presented graphically in Figure 1.

*Table 1: Textural properties of UOP MOLSIV™ PSAO2 XP.*

| Particle diameter (m) | BET surface area (m$^2$/g) | Outer surface area (m$^2$/g) | Micropore area (m$^2$/g) | Pore volume (m$^3$/g) | Micropore volume (m$^3$/g) | Particle porosity (-) | Bulk density (kg/m$^3$) | Particle density (kg/m$^3$) |
|---|---|---|---|---|---|---|---|---|
| 0.002 | 522.8 | 40.2 | 246.7 | $3.47\times10^{-4}$ | $2.47\times10^{-4}$ | 0.38 | 678.96 | 1,095.1 |

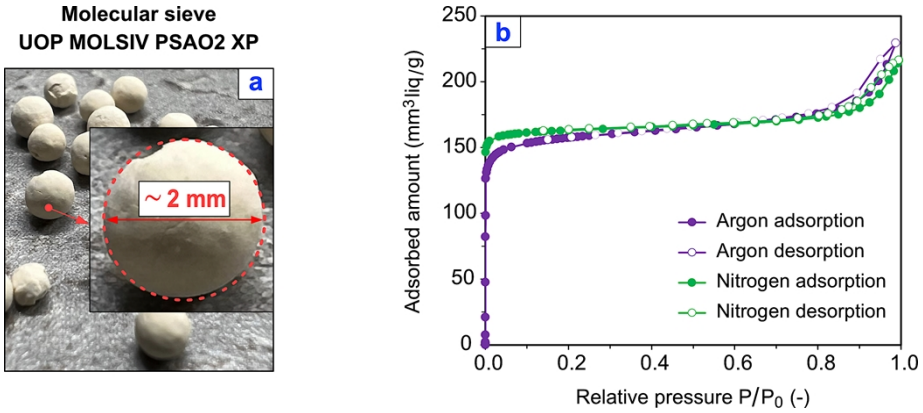


*Figure 1: a) UOP MOLSIV™ PSAO2 XP sample, and b) adsorption isotherms of $N_2$ at 77 K and Ar at 87 K of PSAO2 XP.*

The particle porosity of 0.38 was estimated using Pushnov (2006) correlation for homogeneous solid grain spheres. The particle density was calculated as $\rho_p = \varepsilon_p / V_{pore}$ having a difference of 3.38 % with the bulk density provided by manufacturer, $\rho_b = \rho_p \cdot (1 - \varepsilon_p)$. This difference requires experimental verification. It should be noted that classification by Ar detected a smaller presence of micropores and a smaller BET surface area. Similar differences between results obtained from the Ar and $N_2$ classifications were already observed for microporous zeolite, a difference of 28 % in pore volume (Šolcová et al., 2010); however, since the measurements were not repeated, high consistency with manufacturer data, and selectivity of the adsorbent towards Ar/$N_2$, results of $N_2$ physical adsorption were used. The sample can be classified as microporous; it is relevant to consider the prevailing mass transfer in the interparticle space.

### 2.2 Experimental setup

A two-bed four-step PSA system manufactured by Oxywise s.r.o. is a small-scale on-site oxygen generator. Adsorption takes place in two high-pressure vessels running in parallel with a half-period shift. Figure 2 shows the process flow diagram for air treatment and $O_2$ production, including the experimental laboratory setup and the geometry of the adsorption vessel. Dixon (1988) correlation of packed bed porosity was used to estimate the bed porosity ($\varepsilon_b =$ 0.41), based on the correlation this value can vary up to approximately 10 %, and to determine the weight of the adsorbent in column (8.69 kg).

The process starts by compressing ambient air up to 11 bar, which is subsequently freeze-dried (average dew point temperature of -1 °C), cleaned from dust, oil vapours, and hydrocarbons. Purified air (78 vol. % $N_2$, 21 vol. % $O_2$, 1 vol. % Ar was assumed) is stored in the air storage tank connected to the PSA oxygen generator.

The cyclic $O_2$ production is described for two columns, referred to as **A** and **B**. At the beginning of each cycle, the initial pressure of **A** is 1 bar, and the pressure of **B** is at its highest (6.4 bar). A valve connecting **A** and **B** opens, and **A** is pressurised by the gas exiting **B**, which lasts 19 s on average. The pressure equalization step does not achieve complete equalisation; **A** ends up at about 3 bar, while **B** drops to 3.5 bar. The valve subsequently closes, and **B** is blown down into the atmosphere. It takes 14 s to reach 1 bar. Meanwhile, **A** is undergoing the first stage of pressurisation by high-pressure air from the air storage tank. For 24 s, the $O_2$-enriched gas (product) transfers into the $O_2$ storage tank. During the second half of pressurisation, part of the $O_2$-enriched gas purges **B**, and pressure in **A** increases more gradually. The pressurisation step lasts 48 s; the inlet air flow rate subsequently decreases. Throughout the remaining pressurisation period of **A**, after **B** drops down to 1 bar, **B** remains open to the atmosphere. The process continues in the same way in the reverse order of columns **A** and **B**. A phase shift of one-half characterises two-column systems operating continuously. The duration of one cycle is 134 s, that is, (19 s equalization + 48 s pressurization) × 2.

The air flow rate at 20 °C and pressure of 8.5 - 11 bar ranged from 13 - 17 $m^3$(STP)/h and the product ($O_2$) was obtained at 5 - 7 bar. At different product flow rates, $O_2$ is generated with different purities, which does not affect cycle duration. The sensors continuously measure the flow rates of air fed to the system and the $O_2$ storage tank outlet stream. The adsorption vessel has 1 inlet and 2 outlets (product and waste streams), $O_2$ concentration is measured in each stream.

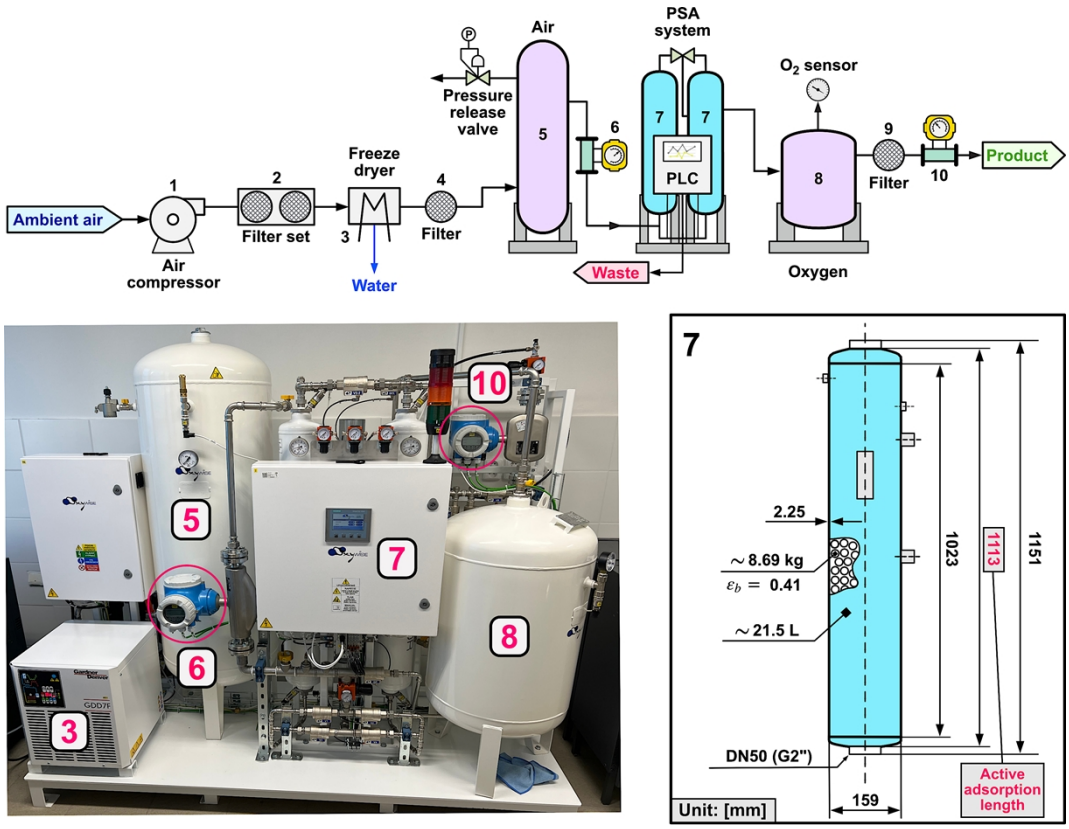


*Figure 2: Process flow diagram from air treatment to $O_2$ production. 1. air compressor, 2. cyclone filter and oil water separator, 3. freeze-dryer, 4. hydrocarbons removal, 5. air storage tank (270 L), 6. air flow meter, 7. PSA $O_2$ generator, 8. $O_2$ storage tank (150 L), 9. bacterial filter, 10. $O_2$ product flowmeter.*

### 2.3 Analytical description of the process

A multicomponent flow balance method was applied to formulate a set of 9 governing equations to calculate the flow rate of each component in each stream entering or exiting the PSA system (9 unknowns). Ambient air is the entering stream, product ($O_2$-enriched gas) and waste ($N_2$-enriched gas) are the exiting streams. The governing equations combine readings from the sensors and assumptions. Specifically, the equations define: the direction and composition of the three streams; the measured amount of inlet air; the measured concentrations of $O_2$ in inlet air, product and waste; the assumed concentration of $N_2$ in inlet air; and the presence of Ar in the product. An exact solution is given by solving equation $\boldsymbol{A}\,\vec{\boldsymbol{x}} = \vec{\boldsymbol{b}}$, where $\boldsymbol{A}$ is the coefficient matrix, $\vec{\boldsymbol{x}}$ is the solution vector (i.e. unknown flow rates of each component) and $\vec{\boldsymbol{b}}$ is the constant vector. The results are used to determine PUR (a measure of product dilution by other components than $O_2$), REC (ratio of $O_2$ present in the product to that in the feed), AirF ( = product stream / (air feed-stream × REC)), BSF (the amount of adsorbent to produce 1 $t_{O2}$/day (Arora and Hasan 2021)), and energy consumption. Furthermore, the model enables verification of the measurement reliability and determination of the sensitivity of individual parameters. Energy consumption was statistically evaluated from a 15-minute measurement period.

## 3. Results and Discussion

Figure 3 shows the pressure history of both PSA columns and the mass flow rate of the purified air fed to the PSA per all cycle steps carried out according to the previous description.

Table 2 presents four intervals of 18 h of collected experimental data in this study that were selected based on the different PUR being constant over 15 min to avoid measurement errors. The cause of errors could be the position of the $O_2$ sensor after the storage tank, which contained a fraction of $O_2$ from previous runs mixing the newly generated $O_2$ and the $O_2$ storage tank was periodically drained to maintain product flow and production rate even. Measurements also revealed suspicious $O_2$ concentrations in the waste stream at high PUR runs. This suggests an improper placement of the other $O_2$ sensor close to the waste outlet where air can be drawn in and the detected gas concentrated from ambient air.

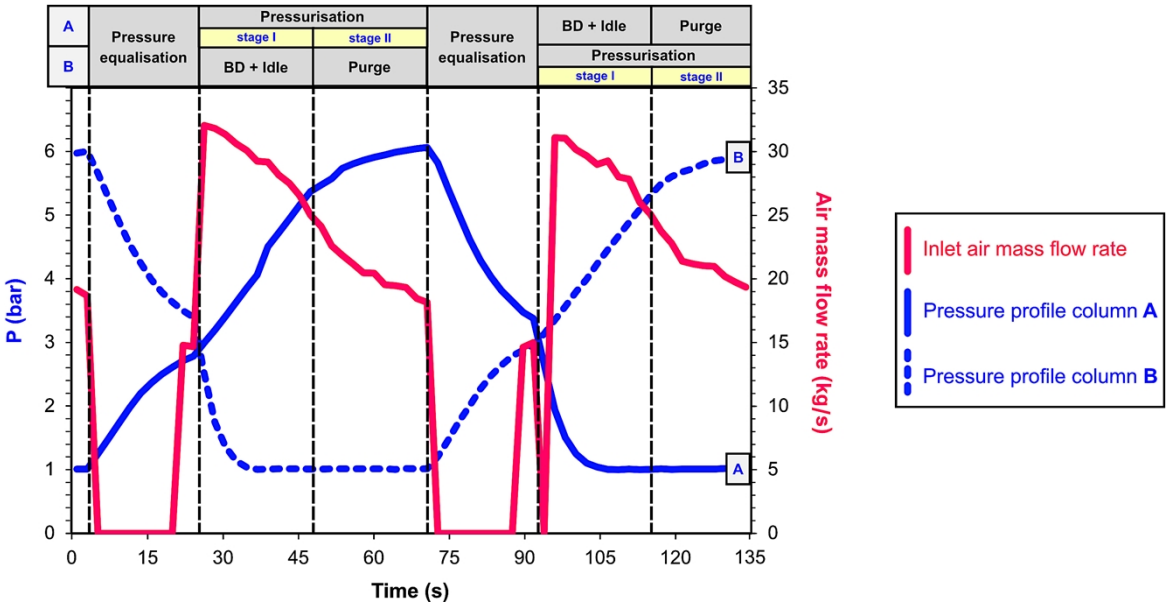


*Figure 3: Pressure profiles of the PSA columns A and B, inlet air mass flow rate.*

*Table 2: Experimental results of the PSA process performance.*

| Cycle no. (-) | Air feed flow rate ($m^3/h$) | PUR (vol. %) | REC (%) | AirF (-) | BSF ($kg_{ads}/(t_{O2}/d)$) | Energy consumption ($MWh/t_{O2}$) |
|---|---|---|---|---|---|---|
| 1 | 17.8 | 66.5 | 47.5 | 6.7 | 277 | 1.097 |
| 2 | 18.1 | 74.6 | 66.8 | 5.3 | 193 | 0.753 |
| 3 | 13.8 | 79.6 | 64.9 | 5.8 | 261 | 0.927 |
| 4 | 17.1 | 94.4 | 20.6 | 21.8 | 625 | 17.389 |

The results are very similar to those overviewed by Arora and Hasan (2021) for medical PSA $O_2$ concentrators. The highest PUR of 95 % showed a significant REC drop, as expected; however, the energy consumption was nearly 20 times higher than that at 80 % PUR, and the AirF almost doubled compared to the commercial data of PSA reported in Šulc and Ditl (2021). Cycle no. 2 has the lowest CAPEX and OPEX given by its BSF (the smallest footprint; production of 1 $t_{O2}/d$ requires 11.5 times larger equipment) and energy consumption, respectively. PUR over 80 % become energy-intensive with a significant leap in energy consumption over 90 % of PUR. Compared to medical units, the determined BSF factor is one order higher, but there is an increased requirement for a small size due to portability reasons. The experimental results provided important data to validate process simulation, which will be the subject of the following study. Therefore, a rigorous numerical model is to be made to enable time-efficient analysis of process performance with as yet untested conditions such as different air flow rate, and experimental data at high PUR to be measured to clearly define a baseline energy consumption for default process parameters, which is a milestone for practical application.

## 4. Conclusions

In this work, PSA $O_2$ generator experiments for obtaining high purity $O_2$ in a single-stage, and classification of PSAO2 XP adsorbent by physical adsorption of $N_2$ and Ar are presented. The physical properties of PSAO2 XP are close to the common NaX-type zeolite, proving its origin. The experiments were carried out to investigate PSA performance in a range of different operating modes and to verify the production of 95 % pure $O_2$. The verification of experiments was approached by designing an analytical model based on the mass flow balances in the system. The optimum operating parameters with the lowest economy are at about 75 % of $O_2$ purity and 65 % recovery. Trade-offs at high purities over 90 % are a large drop in cycle productivity and a steep increment of energy consumption. The purity target of 95 % as an oxidant for oxy-fuel combustion has been achieved; however, the integration of PSA into the oxy-fuel pilot-plant would require larger columns in large numbers due

to high BSF. As the $O_2$ purity corresponding to the optimal cycle is not sufficient for oxy-fuel combustion and the use of PSA in hybrid oxy-fuel combustion, or in combination with other air separation technologies such as polymeric-membranes, it needs to be further investigated.

**Acknowledgements**

This work was supported by the Ministry of Education, Youth and Sports of the Czech Republic under OP RDE grant number CZ.02.1.01/0.0/0.0/16_019/0000753 "Research centre for low-carbon energy technologies". The authors thanks Karel Soukup's Lab (ICPF, Czech Academy of Science) for the adsorbent sample analysis.

**References**

Arora, A., Hasan, M.M.F., 2021, Flexible oxygen concentrators for medical applications, Scientific Reports, 11, 14317.

Banaszkiewicz, T., Chorowski, M., Gizicki, W., 2014, Comparative Analysis of Oxygen Production for Oxy-combustion Application, Energy Procedia, 51, 127–134.

AirSep Corporation, 2013, High Purity PSA Oxygen Systems, <https://files.chartindustries.com/High-Purity-PSA-Oxygen-Systems_MK165-1.pdf> accessed 9.03.2022.

Dixon, A.G., 1988, Correlations for wall and particle shape effects on fixed bed bulk voidage, The Canadian Journal of Chemical Engineering, 66, 705–708.

Gizicki, W., Banaszkiewicz, T., 2020, Performance Optimization of the Low-Capacity Adsorption Oxygen Generator, Applied Sciences, 10, 7495

Krzystowczyk, E., Haribal, V., Dou, J., Li, F., 2021, Chemical Looping Air Separation Using a Perovskite-Based Oxygen Sorbent: System Design and Process Analysis, ACS Sustainable Chemistry & Engineering, 9, 12185–12195.

Linde GmbH, 2019, Oxygen generator plants by Linde, <https://www.linde-engineering.com/en/process-plants/adsorption-and-membrane-plants/oxygen_generation/index.html> accessed 10.03.2022.

Liu, Z., Zhang, T.,2018. Pilot and industrial demonstration of oxy-fuel combustion, Chapter In: Oxy-Fuel Combustion. Elsevier, 209–222.

Micari, M., Agrawal, K.V., 2022, Oxygen enrichment of air: Performance guidelines for membranes based on techno-economic assessment, Journal of Membrane Science, 641, 119883.

Novair Industries, 2019, PSA Twin tower oxygen generators: for medium to high consumption., <https://www.novairindustries.com/en/oxygen-generator/psa> accessed 9.03.2022.

Pushnov, A., 2006, Calculation of average bed porosity, Chemical and Petroleum Engineering, 42, 14–17.

Santos, J.C., Cruz, P., Regala, T., Magalhães, F.D., Mendes, A., 2006, High-Purity Oxygen Production by Pressure Swing Adsorption, Industrial & Engineering Chemistry Research, 46, 591–599.

Skarstrom, C.W., 1960, Method and apparatus for fractionating gas mixtures by adsorption, US Patent No. 2944627.

Skvortsov, S.A., Akulinin, E.I., Golubyatnikov, O.O., Dvoretsky, D.S., Dvoretsky, S.I., 2018, Mathematical modelling of cyclic pressure swing adsorption processes, Journal of Physics: Conference Series, 1015.

Šolcová, O., Matějová, L., Topka, P., Musilová, Z., Schneider, P., 2010, Comparison of textural information from argon (87 K) and nitrogen (77 K) physisorption, Journal of Porous Materials, 18, 557–565.

Šulc, R., Ditl, P., 2021, A technical and economic evaluation of two different oxygen sources for a small oxy-combustion unit, Journal of Cleaner Production, 309, 127427.

Tang, Y., You, F., 2018, Life cycle environmental and economic analysis of pulverized coal oxy-fuel combustion combining with calcium looping process or chemical looping air separation, Journal of Cleaner Production, 181, 271–292.

Texas Compression Services, 2021, Generox® Oxygen Generators for Onsite Use, <https://texascompressionservices.com/oxygen-generators/> accessed 9.03.2022.

Wiessner, F.G., 1988, Basics and industrial applications of pressure swing adsorption (PSA), the modern way to separate gas, Gas Separation & Purification, 2, 115–119.

Wu, F., Argyle, M.D., Dellenback, P.A., Fan, M., 2018, Progress in $O_2$ separation for oxy-fuel combustion - A promising way for cost-effective $CO_2$ capture: A review, Progress in Energy and Combustion Science, 67, 188–205.

Yadav, S., Mondal, S., 2022, A review on the progress and prospects of oxy-fuel carbon capture and sequestration (CCS) technology, Fuel, 308, 122057.